Simulation of complex wave propagation problems using high order parallel finite element methods

1st French-Japanese workshop
Petascale Applications, Algorithms and Programming (PAAP)

Stéphane Lanteri

INRIA, NACHOS project-team
2004 Route des Lucioles, BP 93
06902 Sophia Antipolis Cedex, France
Stephane.Lanteri@inria.fr

INRIA SOPHIA ANTIPOLIS — Université Nice Sophia Antipolis, Laboratoire J. A. Dieudonné — CNRS, Centre National de la Recherche Scientifique

November 1-2 2007
RIKEN Headquarter of Next-Generation Supercomputer R&D Center, Tokyo

Outline

INRIA Sophia Antipolis - Méditerranée

- 530 persons, including 104 researchers, 138 PhD students, 79 engineers, technicians, administrative staff, 46 engineers, 115 post-doctoral students, invited researchers, external specialists
- 150 Foreign scientists (42 different nationalities)
- 30 research project-teams
  - Biological systems
  - Cognitive systems
  - Communicating systems
  - Numerical systems
  - Symbolic systems

INRIA Sophia Antipolis - Méditerranée

- Grid'5000 clusters
  - Cluster of IBM eServer 325
    - AMD Opteron 246, 2.0 GHz (72 dual nodes)
    - 144 cpus x 1 core per cpu = 144 cores
    - Myrinet 2000
  - Cluster of SUN Fire X4100
    - AMD Opteron 275, 2.2 GHz (56 dual nodes)
    - 112 cpus x 2 cores per cpu = 224 cores
    - Myrinet 2000
  - Cluster of Sun Fire X2200 M2
    - AMD Opteron 2218, 2.6 GHz (50 dual nodes)
    - 100 cpus x 2 cores per cpu = 200 cores
    - Gigabit Ethernet
- Production cluster
  - Cluster of IBM eServer 325
    - AMD Opteron 246, 2.0 GHz (64 dual nodes)
    - 128 cpus x 1 cores per cpu = 128 cores
    - Gigabit Ethernet

Outline

Numerical modeling and high performAnce computing
for evolution problems
in Complex domains and HeterogeneOuS media

- Joint team between INRIA, CNRS and University of Nice/Sophia Antipolis via the J.A. Dieudonné Mathematics Laboratory (UMR 6621)
- Official creation in July 2007
- http://www-sop.inria.fr/nachos/index.php/Main/Home

- Permant staff
  - Loula Fezoui [Senior research scientist, INRIA]
    - High order finite volume and finite element methods
    - Computational fluid dynamics, electromagnetics and geoseismics
  - Stéphane Lanteri [Senior research scientist, INRIA], scientific leader
    - High order finite volume and finite element methods
    - Parallel and distributed numerical computing
    - Computational fluid dynamics and electromagnetics
  - Victorita Dolean [Associate professor, University of Nice/Sophia Antipolis]
    - Domain decomposition algorithms
    - Computational fluid dynamics and electromagnetics
  - Francesca Rapetti [Associate professor, University of Nice/Sophia Antipolis]
    - High order finite element methods
    - Domain decomposition algorithms
    - Computational electromagnetics
  - Nathalie Glinsky-Olivier [Research scientist, ENPC[1]]
    - High order finite volume and finite element methods
    - Computational fluid dynamics and geoseismics

[1] École Nationale des Ponts et Chaussées

- Academic collaborations
  - Martin Gander (Mathematics Department, University of Geneva, Switzerland)
  - Frédéric Nataf (Jacques-Louis Lions Laboratory, University of Paris VI)
  - Luc Giraud (ENSEEIHT, Toulouse)
  - Stéphane Operto (CNRS/Géosciences Azur Laboratory, Villefranche sur Mer)
  - Ronan Perrussel (Ecole Centrale de Lyon and CNRS/Ampere Laboratory)
  - Jean Virieux (CNRS/Géosciences Azur Laboratory, Sophia Antipolis)
- Industrial collaborations
  - CEA DAM (Military application division), CESTA center
  - France Telcom R&D, IOP (Interaction of electromagnetic wave with humans) team, Joe Wiart

- Design, analysis et validation of numerical methods and high performance resolution algorithms for the computer simulation of evolution problems in complex domains and heterogeneous media
- Focus on linear systems of PDEs with variable coefficients
- Time-domain problems

$$\mathbf{x} \in \Omega \subset \boldsymbol{R}^d \quad , \quad t \in \boldsymbol{R}^+ \quad : \quad \frac{\partial U}{\partial t} + \sum_{i=1}^{d} A_i(\mathbf{x}) \frac{\partial U}{\partial x_i} = S(\mathbf{x}, t)$$

- Time-harmonic problems

$$\mathbf{x} \in \Omega \subset \boldsymbol{R}^d \quad , \quad \omega \in \boldsymbol{R}^+ \quad : \quad i\omega U + \sum_{i=1}^{d} A_i(\mathbf{x}) \frac{\partial U}{\partial x_i} = S(\mathbf{x}, \omega)$$

- The matrices $A_i(\mathbf{x})$ characterize the media
- Could be $A_i(\mathbf{x}, t)$ or $A_i(\mathbf{x}, \omega)$ as well

- Computational electromagnetics
  - Maxwell equations
    - Dispersion and/or physical dissipation models for complex materials e.g biological tissues (time-domain Maxwell equations)
    - Diffraction of monochromatic waves by complex and heterogeneous objects (time-domain and time-harmonic Maxwell equations)
    - Interaction of charged particles with electromagnetic fields (time-domain Vlasov/Maxwell equations coupling)
- Computational geoseismics
  - Elastodynamic equations
    - Propagation of elastic waves in materials with variable geological characteristics
    - Numerical modeling of planar and non-planar faults i.e regions with known and well documented seismic activity

- Computational electromagnetics
  - Maxwell equations
    - Dispersion and/or physical dissipation models for complex materials e.g biological tissues (time-domain Maxwell equations)
    - Diffraction of monochromatic waves by complex and heterogeneous objects (time-domain and time-harmonic Maxwell equations)
    - Interaction of charged particles with electromagnetic fields (time-domain Vlasov/Maxwell equations coupling)
- Computational geoseismics
  - Elastodynamic equations
    - Propagation of elastic waves in materials with variable geological characteristics
    - Numerical modeling of planar and non-planar faults i.e regions with known and well documented seismic activity

- Accuracy
  - High order discontinuous Galerkin (DG) methods on simplex meshes
  - Conforming and non-conforming *hp*-adaptivity
  - Numerical treatment of complex material models
- Numerical efficiency
  - Hybrid explicit/implicit time integration strategies
  - Domain decomposition algorithms
    - Parallel linear system solvers or parallel preconditioning methods
    - Algorithms that couple different discretization methods working on different mesh types
    - Algorithms that couple different physical models
- Computational efficiency
  - Parallelization strategies for unstructured mesh based numerical methods
  - Load balancing issues for adaptive DG methods
  - Hierachical SPMD parallel programming model

Outline

Discontinuous Galerkin (DG) methods

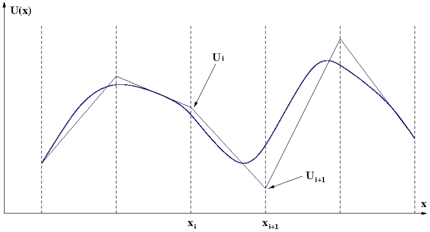

FE, continuous P1 interpolation

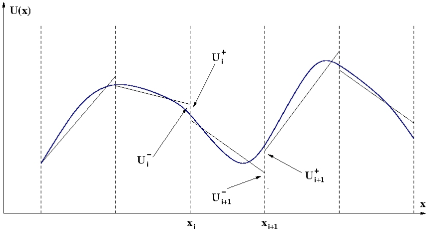

DG, local P1 interpolation

- Can easily deal with discontinuous coefficients and solutions
- Can handle unstructured, non-conforming meshes
- Yield local finite element mass matrices
- High order accurate methods with compact stencils
- Naturally lead to discretization (h-) and interpolation order (p-) adaptivity
- Amenable to efficient parallelization

Discontinuous Galerkin (DG) methods

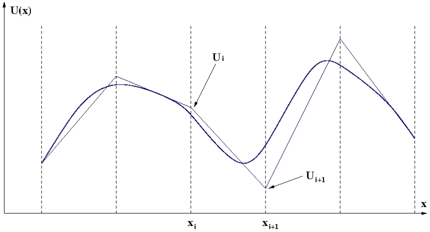

FE, continuous P1 interpolation

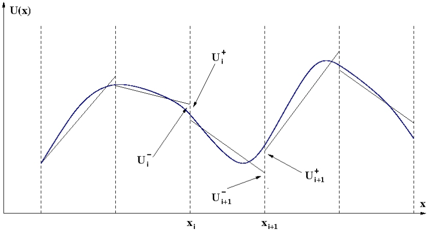

DG, local P1 interpolation

- Can easily deal with discontinuous coefficients and solutions
- Can handle unstructured, non-conforming meshes
- Yield local finite element mass matrices
- High order accurate methods with compact stencils
- Naturally lead to discretization (h-) and interpolation order (p-) adaptivity
- Amenable to efficient parallelization

- Problem to solve

  $\mathbf{x} \in \Omega \subset \boldsymbol{R}^d$, $t \in \boldsymbol{R}^+$, $u = u(\mathbf{x}, t)$, $a_i = a_i(\mathbf{x})$ scalar real functions

$$\frac{\partial u}{\partial t} + \sum_{i=1}^{d} a_i \frac{\partial u}{\partial x_i} = 0 \tag{1}$$

- Weak formulation

$$< \frac{\partial u}{\partial t}, \ v >_\Omega + \sum_{i=1}^{d} < a_i \frac{\partial u}{\partial x_i}, \ v >_\Omega = 0 \tag{2}$$

$< u \ , \ v >_\Omega = \displaystyle\int_\Omega uv d\mathbf{x}$, v being a *test function*

Discontinuous Galerkin (DG) methods
Basic formulation

- Galerkin method
  - $\tau_h = \{K\}$ triangulation of Ω
  - $P^m(K)$: polynomials of degree at most m on K

For each $K \in \tau_h$ find $u^h : u^h|_K \in P^m(K)$ such that:

$$< \frac{\partial u^h}{\partial t}, \; v >_K + \sum_{i=1}^{d} < a_i \frac{\partial u^h}{\partial x_i}, \; v >_K = 0 \quad , \forall v \in P^m(K) \tag{3}$$

Integrating by parts (setting $a|_K \in P^0(K)$)

$$\begin{aligned} < \frac{\partial u^h}{\partial x_i}, \; v >_K &= - < u^h, \; \frac{\partial v}{\partial x_i} >_K + < u^h n_i, \; v >_{\partial K} \\ < u, \; v >_{\partial K} &= \sum_{j=1}^{N_f(K)} < u, \; v >_{\partial K \cap \partial K_j} \end{aligned}$$

- $\mathbf{n} = \{n_i\}$ outward unit normal of ∂K
- $N_f(K)$ = number of faces of K

- Discontinous approximation: $u^h|_{K\cap K_j}$ not well defined!

  $\Rightarrow$ Centered approximation: $u^h(\hat{\mathbf{x}}) = \dfrac{u^h|_K(\hat{\mathbf{x}}) + u^h|_{K_j}(\hat{\mathbf{x}})}{2}$, $\forall \hat{\mathbf{x}} \in K \cap K_j$

- Linear algebra

  - $u^h|_K(\mathbf{x},t) = \sum_{j=1}^{m_K} u^h_{j,K}(t)\psi_{j,K}(\mathbf{x})$, $m_K = \dim(P^m(K))$
  - $\{\psi_{j,K}\}, j = 1,\ldots,m_K$: basis of $P^m(K)$

$$\mathbf{M}_K \frac{\partial \mathbf{U}^h_K}{\partial t} = \sum_{i=1}^{d} a_i \left(\mathbf{R}_{i,K}\mathbf{U}^h_K - n_i \sum_{j=1}^{N_f(K)} \mathbf{S}_{K,K_j}\mathbf{U}^h_K \right)$$

$$\begin{array}{lcl}
\mathbf{U}^h_K & = & \mathbf{U}^h_K(t) = \{u^h_{j,K}(t)\}, \;\; j = 1,\ldots,m_K \\
\mathbf{M}_K[l,m] & = & <\psi_{l,K},\ \psi_{m,K}>_K \\
\mathbf{R}_{i,K}[l,m] & = & <\dfrac{\partial \psi_{l,K}}{\partial x_i},\ \psi_{m,K}>_K \\
\mathbf{S}_{K,K_j}[l,m] & = & <\psi_{l,K},\ \psi_{m,K_j}>_{\partial K \cap \partial K_j}
\end{array}$$

Dimension of local systems: $m_K \times m_K$

Discontinuous Galerkin (DG) methods

- Arguments for flexibility
  - Type of approximation (polynomial, trigonometric, etc.)
  - *p*-adaptivity (approximation is purely local)
  - *h*-adaptivity (conforming or non-conforming grid refinement)
  - Time integration scheme
- Computational aspects
  - Increased number of degrees of freedom (with regards to continuous finite element methods)
  - Extensive use of BLAS 2 operations

Outline

The system of Maxwell equations

$$\text{In } \Omega \subset \mathbb{R}^3 \; : \; \left\{ \begin{array}{rcrcl} \varepsilon(\mathbf{x})\mathcal{F}(\mathbf{E}) & - & \nabla \times \mathbf{H} & = & -\mathbf{J} \\ \mu(\mathbf{x})\mathcal{F}(\mathbf{H}) & + & \nabla \times \mathbf{E} & = & 0 \end{array} \right.$$

- Time-domain formulation
  - $\mathbf{E} = \mathbf{E}(\mathbf{x}, t)$, $\mathbf{H} = \mathbf{H}(\mathbf{x}, t)$ and $\mathbf{J} = \mathbf{J}(\mathbf{x}, t)$
  - $\mathcal{F}(\mathbf{E}) = \dfrac{\partial \mathbf{E}}{\partial t}$ and $\mathcal{F}(\mathbf{H}) = \dfrac{\partial \mathbf{H}}{\partial t}$
- Time-harmonic formulation
  - $\mathbf{E} = \mathbf{E}(\mathbf{x}, \omega)$, $\mathbf{H} = \mathbf{H}(\mathbf{x}, \omega)$ and $\mathbf{J} = \mathbf{J}(\mathbf{x}, \omega)$
  - $\mathcal{F}(\mathbf{E}) = \mathrm{i}\omega\mathbf{E}$ and $\mathcal{F}(\mathbf{H}) = \mathrm{i}\omega\mathbf{H}$
- Conductive media: $\mathbf{J} = \sigma(\mathbf{x})\mathbf{E}$ with electric conductivity $\sigma(\mathbf{x})$
- Boundary conditions
  - Perfect electric conductor condition: $\vec{n} \times \mathbf{E} = 0$
  - Silver-Müller (first order absorbing boundary) condition:

$$\vec{n} \times \mathbf{E} - \vec{n} \times (\mathbf{H} \times \vec{n}) = (\vec{n} \times \mathbf{E}^{\mathrm{inc}} - \vec{n} \times (\mathbf{H}^{\mathrm{inc}} \times \vec{n}))$$

Discontinuous Galerkin time-domain methods

- Unstructured tetrahedral meshes
- Based on $\mathbb{P}_p$ nodal (Lagrange) interpolation
  - $\mathbb{P}_0$-DGTD method: 6 dof per tetrahedron (FVTD method)
  - $\mathbb{P}_1$-DGTD method: 24 dof per tetrahedron
  - $\mathbb{P}_2$-DGTD method: 60 dof per tetrahedron
  - etc.
- Centered fluxes for the calculation of jump terms at cell boundaries
- Leap-frog time integration
- Theoretical aspects
  - L. Fezoui, S. Lanteri, S. Lohrengel and S. Piperno
    M2AN, Vol. 39, No. 6, 2005
  - Conditional stability (conservation of a discrete electromagnetic energy)
  - Convergence: $\mathcal{O}(Th^{\min(s,p)}) + \mathcal{O}(\Delta t^2)$
- Computational aspects: SPMD parallelization strategy
  - Mesh partitioning (ParMeTiS) + message passing model (MPI)
  - M. Bernacki, S. Lanteri and S. Piperno
    Appl. Math. Model., Vol. 30, No. 8, 2006.

- Monochromatic wave, F=1 GHz
  - Mesh M1: # vertices = 75,200 , # tetrahedra = 423,616
  - $L_{\text{min}} = 0.000601$ m , $L_{\text{max}} = 0.144679$ m $(\approx \dfrac{\lambda}{0.5})$, $L_{\text{avg}} = 0.041361$ m

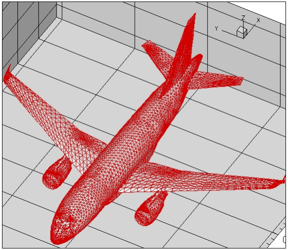

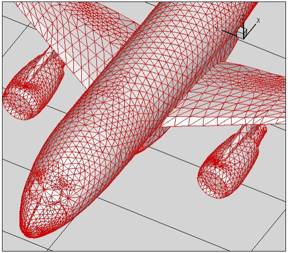

- Monochromatic wave, F=1 GHz
  - Mesh M1: # vertices = 75,200 , # tetrahedra = 423,616
  - $L_{\text{min}} = 0.000601$ m , $L_{\text{max}} = 0.144679$ m $(\approx \dfrac{\lambda}{0.5})$, $L_{\text{avg}} = 0.041361$ m

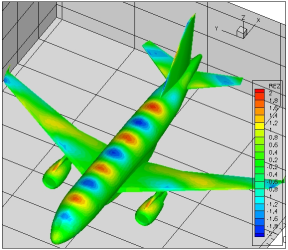

$\mathbb{P}_1$-DGTD method

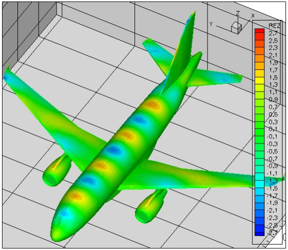

$\mathbb{P}_2$-DGTD method

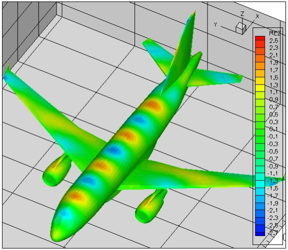

$\mathbb{P}_3$-DGTD method

Contour lines of the real part of DFT(E_z)

- Performance results
  - AMD Opteron/2 GHz, Gigabit Ethernet

Method	N_p	CPU (min/max)	REAL	% CPU
$\mathbb{P}_1$-DGTD	32	38 mn/38 mn	40 mn	98.5%
$\mathbb{P}_2$-DGTD	32	2 h 20 mn/2 h 33 mn	2 h 35 mn	98.5%
$\mathbb{P}_3$-DGTD	32	4 h 49 mn/5 h 08 mn	5 h 12 mn	99.0%

- A multi-disciplinary cooperative research action
  - Medical image processing, geometrical modeling and numerical modeling
- Objectives
  - Contribute to ongoing research activities on biological effects resulting from the use of mobile phones
  - Demonstrate the benefits of using unstructured mesh Maxwell solvers for numerical dosimetric studies
  - Evaluate the thermal effects induced by the electromagnetic radiation in head tissues
- Specific activities
  - Medical image processing (segmentation of head tissues)
  - Geometric modeling (surface and volumic mesh generation)
  - Numerical modeling (time domain Maxwell solvers, bioheat equation solver)
  - Experimental validations

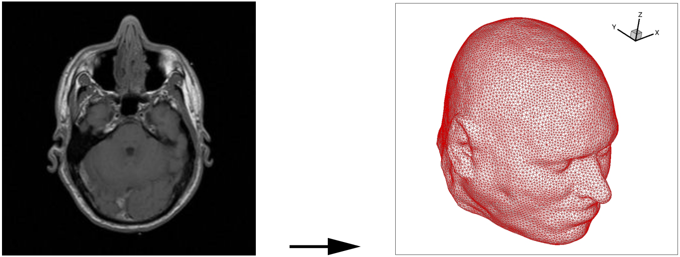

- Geometric models
  - Built from segmented medical images
  - Extraction of surfacic (triangular) meshes of the tissue interfaces using specific tools
    - Marching cubes + adaptive isotropic surface remeshing (P. Frey, 2001)
    - Delaunay refinement (J.-D. Boissonnat and S. Oudot, 2005)
    - Level-set method (J.-P. Pons, 2005)
  - Generation of tetrahedral meshes using a Delaunay/Voronoi tool

Characteristics of tissues (F=1800 MHz)
Wavelength λ in air: 166.66 mm

Tissue	ε_r	σ (S/m)	ρ (Kg/m^3)	λ (mm)
Skin	43.85	1.23	1100.0	26.73
Skull	15.56	0.43	1200.0	42.25
CSF	67.20	2.92	1000.0	20.33
Brain	43.55	1.15	1050.0	25.26

Characteristics of unstructured meshes of head tissues

- Coarse mesh (M1)
  - # vertices = 135,633 and # tetrahedra = 781,742

Tissue	L_{min} (mm)	Lmax (mm)	Lmoy (mm)	λ (mm)
Skin	1.339	8.055	4.070	26.73
Skull	1.613	7.786	4.069	42.25
CSF	0.650	7.232	4.059	20.33
Brain	0.650	7.993	4.009	25.26

- Fine mesh (M2)
  - # vertices = 889,960 and # tetrahedra = 5,230,947

Tissue	L_{min} (mm)	Lmax (mm)	Lmoy (mm)	λ (mm)
Skin	0.821	5.095	2.113	26.73
Skull	0.776	4.265	2.040	42.25
CSF	0.909	3.701	1.978	20.33
Brain	0.915	5.509	2.364	25.26

Discontinuous Galerkin time-domain methods

Intreraction of electromagnetic waves with biological tissues

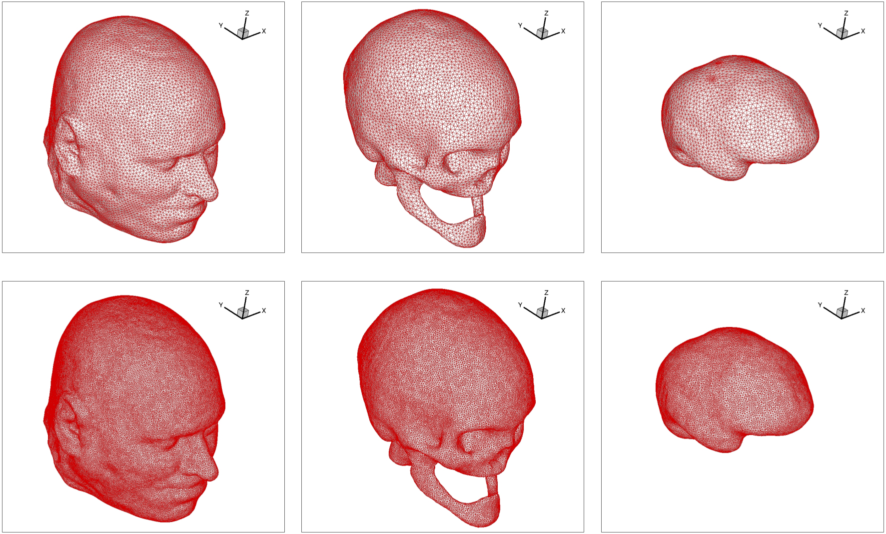

HeadExp collaborative research action

Head + simplified telephone model

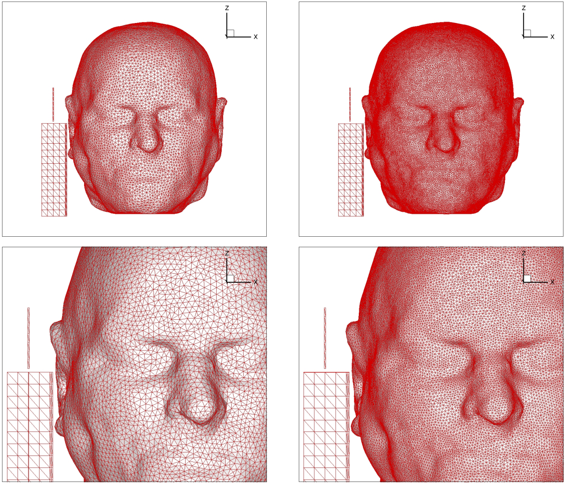

Characteristics of unstructured meshes
Head tissues + telephone + free space

- Coarse mesh (M1)
  - # vertices = 311,259 and # tetrahedra = 1,862,136
  - Time step: 0.653 psec ($\mathbb{P}_0$-DGTD method) and 0.019 psec ($\mathbb{P}_1$-DGTD method)

$L_{\min}$ (mm)	$L_{\max}$ (mm)	L_{moy} (mm)
0.650	8.055	4.064

- Fine mesh (M2)
  - # vertices = 1,308,842 and # tetrahedra = 7,894,172
  - Time step: 0.663 psec ($\mathbb{P}_0$-DGTD method)

$L_{\min}$ (mm)	$L_{\max}$ (mm)	L_{moy} (mm)
0.776	5.509	2.132

SAR (Specific Absorption Rate) : $\dfrac{\sigma|\mathbf{E}|^2}{\rho}$

SAR/SARmax (log scale)

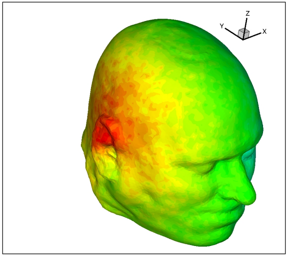

Mesh M1, $\mathbb{P}_0$-DGTD method

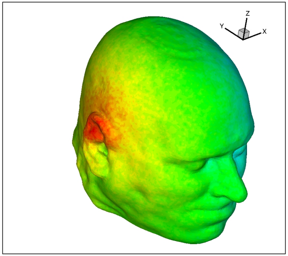

Mesh M2, $\mathbb{P}_0$-DGTD method

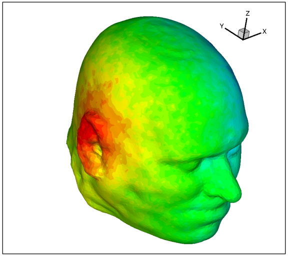

Mesh M1, $\mathbb{P}_1$-DGTD method

SAR (Specific Absorption Rate) : $\frac{\sigma|\mathbf{E}|^2}{\rho}$

SAR/SARmax (log scale)

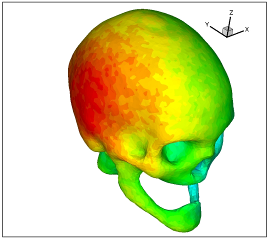

Mesh M1, $\mathbb{P}_0$-DGTD method

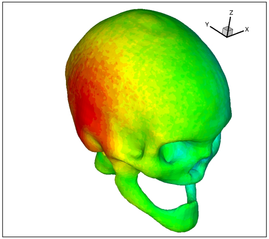

Mesh M2, $\mathbb{P}_0$-DGTD method

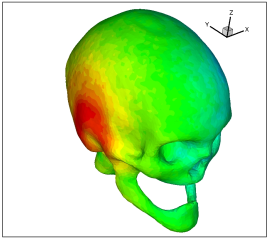

Mesh M1, $\mathbb{P}_1$-DGTD method

SAR (Specific Absorption Rate) : $\dfrac{\sigma|\mathbf{E}|^2}{\rho}$

SAR/SARmax (log scale)

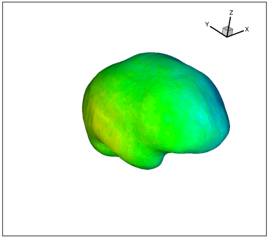

Mesh M1, $\mathbb{P}_0$-DGTD method

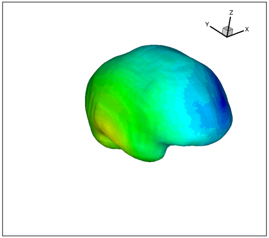

Mesh M2, $\mathbb{P}_0$-DGTD method

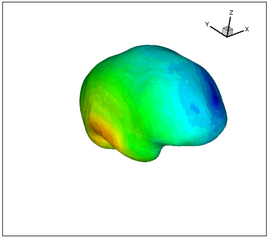

Mesh M1, $\mathbb{P}_1$-DGTD method

Discontinuous Galerkin time-domain methods

Intreraction of electromagnetic waves with biological tissues

Electric field amplitude $|\mathbf{E}|$ (log sacle)

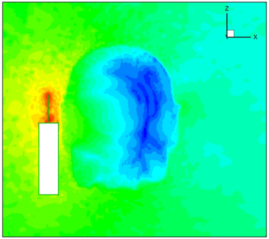

Mesh M1, $\mathbb{P}_0$-DGTD method

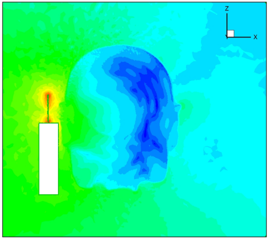

Mesh M2, $\mathbb{P}_0$-DGTD method

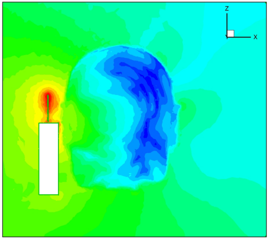

Mesh M1, $\mathbb{P}_1$-DGTD method

Mesh	Method	Local SAR (W/Kg)	SAR_{1g} (W/Kg)	SAR_{10g} (W/Kg)
M1	$\mathbb{P}_0$-DGTD	104.3	37.7	19.5
-	$\mathbb{P}_1$-DGTD	23.8	15.0	9.1
M2	$\mathbb{P}_0$-DGTD	309.9	53.8	22.4

Normalized peak SAR values

Mesh	Mehod	N_p	CPU	REAL	% CPU	$S(N_p)$
M1	$\mathbb{P}_0$-DGTD	32	36 mn	39 mn	92%	-
-	$\mathbb{P}_1$-DGTD	32	6 h 32 mn	6 h 48 mn	95%	-
M2	$\mathbb{P}_0$-DGTD	32	2 h 46 mn	2 h 54 mn	95%	1.00
-	-	64	1 h 20 mn	1 h 25 mn	94%	2.00

Cluster of AMD Opteron/2.0 GHz nodes, Gigabit Ethernet

- Future works
  - In collaboration with France Telcom R&D, IOP (Interaction of electromagnetic wave with humans) team, Joe Wiart
    - High order $\mathbb{P}_p$-DGTD methods on locally refined, non-conforming tetrahedral meshes
    - Numerical treatment of dispersive material models with DGTD methods
    - Application to full body exposure
  - Generalization to other applications (medical domain)

Full body exposure to a plane wave (# vertices = 899,872 and # tetrahedra = 5,335,521)

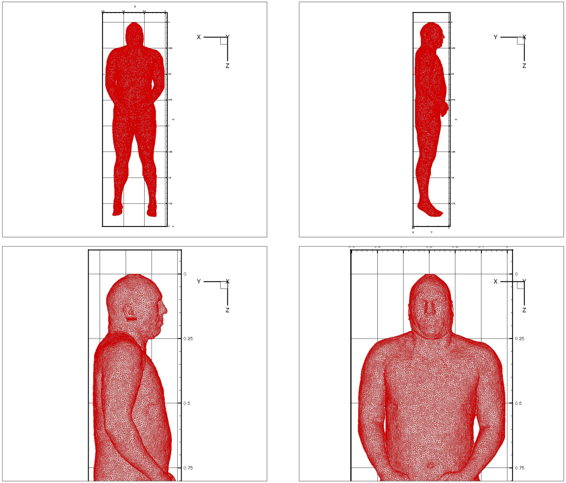

Full body exposure to a plane wave (# vertices = 899,872 and # tetrahedra = 5,335,521)

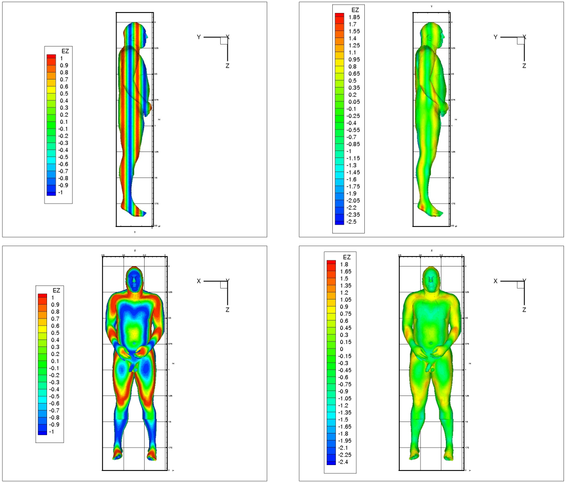

F=2140 MHz, $\mathbb{P}_1$-DGTD method: $\varepsilon_r = 1$ (left) and $\varepsilon_r = 2$ (right)

Discontinuous Galerkin time-harmonic methods
$\mathbb{P}_p$-DGTH formulation

- Unstructured triangular (2D)/tetrahedral (3D) meshes
- Based on $\mathbb{P}_p$ nodal (Lagrange) interpolation
  - Implementation in the 3D case
    - $\mathbb{P}_0$-DGTD method: 6 dof per tetrahedron
    - $\mathbb{P}_1$-DGTD method: 24 dof per tetrahedron
- Centered or upwind fluxes for the calculation of jump terms at cell boundaries
- Theoretical aspects
  - H. Fol (PhD thesis, december 2006)
  - V. Dolean, H. Fol, S. Lanteri and R. Perrussel (submitted, 2007)
  - Well-posedness (invertibility) of the discrete system
- Computational aspects: SPMD parallelization strategy
  - Mesh partitioning (ParMeTiS) + message passing model (MPI)
  - Iterative and direct linear system solvers
  - Domain decomposition solver (hybrid iterative/direct)

- Numerical convergence in the 2D case (triangular meshes)

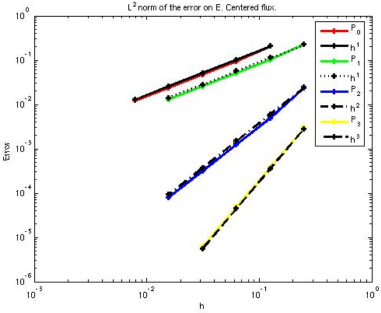

Centered flux

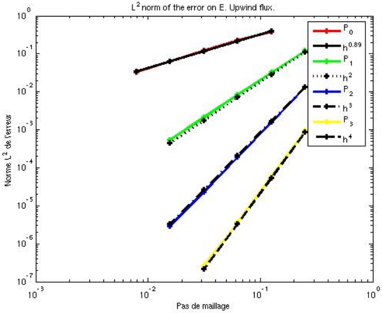

Upwind flux

Flux	$\mathbb{P}_0$	$\mathbb{P}_1$	$\mathbb{P}_2$	$\mathbb{P}_3$
Centered	1.02	1.03	2.05	2.97
Upwind	0.89	1.95	3.03	3.95

Discontinuous Galerkin time-harmonic methods

Domain decomposition solver

- Time-harmonic Maxwell system: $\mathcal{L}\mathbf{W} = \mathrm{i}\omega\mathbf{G}_0\mathbf{W} + \mathbf{G}_x\partial_x\mathbf{W} + \mathbf{G}_y\partial_y\mathbf{W} + \mathbf{G}_z\partial_z\mathbf{W}$
- Schwarz algorithm: $\Omega = \bigcup_{j=1}^{m}\Omega_j$, $\mathbf{W}^j = \mathbf{W}|_{\Omega_j}$

$$\left\{\begin{array}{rcl} \mathcal{L}\mathbf{W}^{j,p+1} & = & \mathbf{f}^j \text{ in } \Omega_j \\ \mathbf{G}^-_{\vec{n}_{jl}}\mathbf{W}^{j,p+1} & = & \mathbf{G}^-_{\vec{n}_{jl}}\mathbf{W}^{l,p} \text{ on } \Gamma_{jl} = \partial\Omega_j \cap \bar{\Omega}_l \\ \mathbf{G}^-_{\vec{n}}\mathbf{W}^{j,p+1} & = & \mathbf{G}^-_{\vec{n}}\mathbf{W}_{\mathrm{inc}} \text{ on } \Omega \cap \Omega_j \end{array}\right.$$

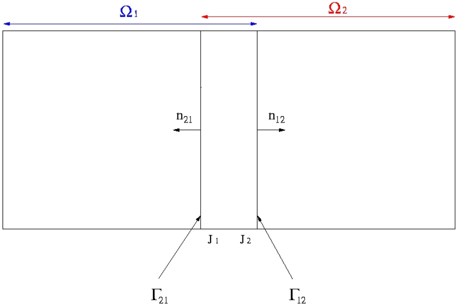

- Schwarz algorithm: convergence analysis
  - Two dimensional case
  - Two subdomain case: $\Omega_1 =]-\infty, b[\times\mathbb{R}$ and $\Omega_2 =]a, +\infty[\times\mathbb{R}$ with $a \leq b$
  - Fourier analysis

$$\widehat{\mathbf{E}}^{j,p}(x,k) = (\mathcal{F}_y \mathbf{E}^{j,p})(x,k) = \int_{\mathbb{R}} e^{-iky} \mathbf{E}^{j,p}(x,y)\, dy$$

with $\mathbf{E}^{j,p} = \mathbf{U}^{j,p} - \mathbf{U}_{|\Omega_j}$ and $\mathbf{U} = \mathbf{T}^{-1}\mathbf{W}$

  - Convergence rate

$$\rho(k,\delta) = \left| \left(\frac{\sqrt{k^2-\omega^2} - \mathrm{i}\omega}{\sqrt{k^2-\omega^2} + \mathrm{i}\omega} \right) e^{-\delta\sqrt{k^2-\omega^2}} \right|$$

with $\delta = b - a$

  - Convergence of the Schwarz algorithm: $\forall\, k \in \mathbb{R},\ \rho(k,\delta) < 1$

$$\rho(k,\delta) = \begin{cases} \left| \dfrac{\sqrt{\omega^2-k^2} - \omega}{\sqrt{\omega^2-k^2} + \omega} \right| & \text{si } |k| < \omega \quad \text{(propagative modes)} \\ e^{-\delta\sqrt{k^2-\omega^2}} & \text{si } |k| \geq \omega \quad \text{(evanescent modes)} \end{cases}$$

- Schwarz algorithm: convergence analysis

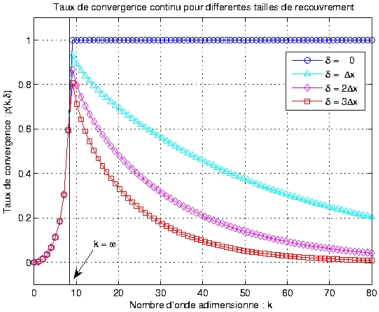

F=400 MHz

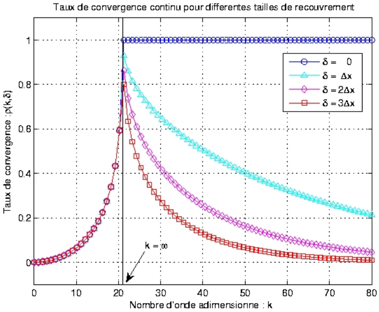

F=1 GHz

- Schwarz algorithm: algorithmic aspects
  - Global system (two-sudomain case)

$$\begin{pmatrix} A_1 & 0 & R_1 & 0 \\ 0 & A_2 & 0 & R_2 \\ 0 & -B_2 & \mathrm{Id} & 0 \\ -B_1 & 0 & 0 & \mathrm{Id} \end{pmatrix} \begin{pmatrix} \mathbf{W}_h^1 \\ \mathbf{W}_h^2 \\ \lambda_h^1 \\ \lambda_h^2 \end{pmatrix} = \begin{pmatrix} \mathbf{f}_h^1 \\ \mathbf{f}_h^2 \\ \mathbf{0} \\ \mathbf{0} \end{pmatrix}$$

  - Interface system: $\mathcal{T}_h \lambda_h = \mathbf{g}_h$

$$\mathcal{T}_h = \begin{pmatrix} \mathrm{Id} & B_2 A_2^{-1} R_2 \\ B_1 A_1^{-1} R_1 & \mathrm{Id} \end{pmatrix} \quad \text{and} \quad \mathbf{g}_h = \begin{pmatrix} B_2 A_2^{-1} F^2 \\ B_1 A_1^{-1} F^1 \end{pmatrix}$$

    - Schwarz iteration $\Leftrightarrow \lambda_h^{p+1} = (\mathrm{Id} - \mathcal{T}_h)\lambda_h^p + \mathbf{d}_h$
    - Accelerated iteration: Krylov method

- Schwarz algorithm: numerical and parallel performances
  - Diffraction of a plane wave (F=1800 MHz)
  - Model (artificial) problem

Tissue	ε_r	σ (S/m)	ρ (Kg/m^3)	λ (mm)
Skin	4.0	0.0	1100.0	26.73
Skull	1.5	0.0	1200.0	42.25
CSF	6.5	0.0	1000.0	20.33
Brain	4.0	0.0	1050.0	25.26

  - Characteristics of the tetrahedral meshes (no telephone model)

Mesh	# vertices	# tetrahedra	L_{min} (mm)	Lmax (mm)	Lavg (mm)
M1	60,590	361,848	1.85	45.37	11.65
M2	309,599	1,853,832	1.15	24.76	6.93

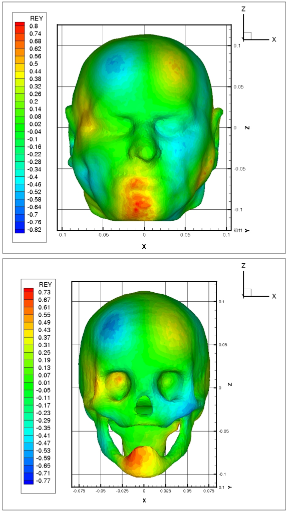

Mesh M2, $\mathbb{P}_0$-DGTH method

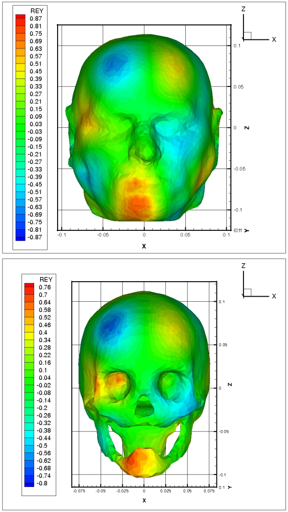

Mesh M1, $\mathbb{P}_1$-DGTH-c method

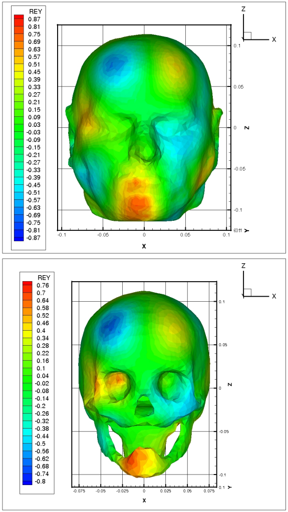

Mesh M1, $\mathbb{P}_1$-DGTH-u method

- Interface system
  - BiCGstab(ℓ) (G.L.G. Sleijpen and D.R. Fokkema, ETNA, Vol.1, 1993)
  - No preconditioner, $\ell = 6$
- Local systems
  - MUMPS multifrontal sparse solver
    (P.R. Amestoy, I.S. Duff and J.-Y. L'Excellent
    Comput. Meth. App. Mech. Engng., Vol 184, 2000)
  - L and U factors in 32 bit accuracy

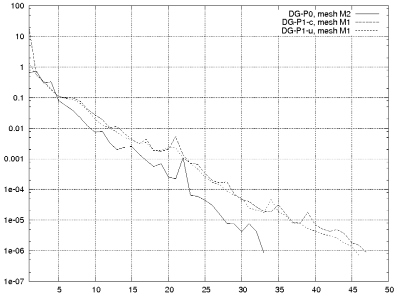

- Cluster of AMD Opteron/2.6 GHz nodes, Gigabit Ethernet/Myrinet
  - DG-$\mathbb{P}_1$-c: DGTH method with centered flux
  - DG-$\mathbb{P}_1$-u: DGTH method with upwind flux

Mesh	Method	Strategy	N_s	# it	CPU (min/max)	REAL
M1	DG-$\mathbb{P}_1$-c	DD-itref	96	47	346 sec/466 sec	714 sec
-	-	-	-	-	524 sec/715 sec	717 sec
-	DG-$\mathbb{P}_1$-u	DD-itref	96	47	347 sec/547 sec	765 sec
-	-	-	-	-	636 sec/685 sec	686 sec
M2	DG-$\mathbb{P}_0$-c	DD-itref	48	27	545 sec/770 sec	1350 sec
-	-	-	96	33	228 sec/322 sec	428 sec
-	-	-	-	-	415 sec/416 sec	417 sec

Mesh	Method	N_s	CPU (min/max)	RAM (min/max)	# dof
M1	DG-$\mathbb{P}_1$-c	96	64 sec/125 sec	640 MB/852 MB	8,684,352
-	DG-$\mathbb{P}_1$-u	96	80 sec/134 sec	633 MB/866 MB	-
M2	DG-$\mathbb{P}_0$-c	48	234 sec/374 sec	1432 MB/1836 MB	11,122,992
-	-	96	53 sec/ 98 sec	519 MB/ 684 MB	-

- Future works
  - Schwarz algorithms based on optimized interface conditions
  - Extension to time-domain problems time integrated using implicit schemes
  - Algebraic preconditioning of the interface system
    (in collaboration with Luc Giraud and Azzam Haidar, Parallel Algorithms and Optimization Group, ENSEEIHT, Toulouse)

Outline

Overall objectives

- Development of high order DG methods on triangular (2D case) and tetrahedral (3D case) meshes for dynamic fault rupture
- Comparison with state of the art numerical methods (finite difference methods on cartesian meshes, boundary element method)
- Collaborations
  - Jean Virieux (University of Nice/Sophia Antipolis and GéoSciences Azur Laboratory)
  - Victor Manuel Cruz-Atienza (Department of Geological Sciences San Diego State University)

The system of elastodynamic equations

- Velocity/stress formulation

$$\text{In} \quad \Omega \subset \mathbb{R}^3 \quad : \quad \left\{ \begin{array}{rcl} \rho(\mathbf{x})\dfrac{\partial \mathbf{v}}{\partial t} & = & \overrightarrow{\text{div}\,\underline{\sigma}} = 0 \\ \dfrac{\partial \underline{\sigma}}{\partial t} & = & \lambda(\mathbf{x})(\text{div}\,\mathbf{v})\text{Id} + \mu(\mathbf{x})\left[\nabla \mathbf{v} +^t (\nabla \mathbf{v})\right] \end{array} \right.$$

with:

$$\underline{\sigma} = \begin{pmatrix} \sigma_{xx} & \sigma_{xy} & \sigma_{xz} \\ \sigma_{xy} & \sigma_{yy} & \sigma_{yz} \\ \sigma_{xz} & \sigma_{yz} & \sigma_{zz} \end{pmatrix} \quad \text{and} \quad \mathbf{v} = \begin{pmatrix} v_x \\ v_y \\ v_z \end{pmatrix}$$

- Boundary conditions
  - Artificial boundary: first order absorbing boundary condition
  - Free surface: $\underline{\sigma} = 0$
  - Dynamic fault: ${}^t\mathbf{n}\,\underline{\sigma}\,\mathbf{t} = g(t)$

Finite volume method

- Unstructured triangular (2D) and tetrahedral (3D) meshes
- $\mathbb{P}_0$-DGTD method
  - 2D case: 5 dof per traingle
  - 3D case: 9 dof per tetrahedron
- Centered fluxes for the calculation of jump terms at cell boundaries
- Leap-frog time integration
- N. Glinsky-Olivier, M. Ben Jemaa, J. Virieux and S. Piperno
  2D seismic wave propagation by a finite volume method
  68th EAGE Conference & Exhibition, Vienna, Austria, 2006
- Computational aspects: SPMD parallelization strategy
  - Mesh partitioning (ParMeTiS) + message passing model (MPI)

Numerical results: propagation

Seismic wave propagation: corner edge

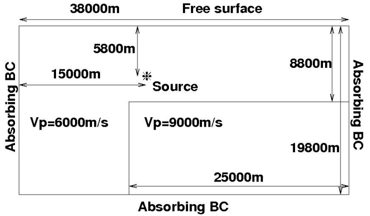

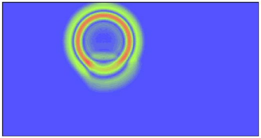

t=1.0 s

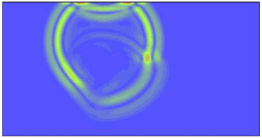

t=1.5 s

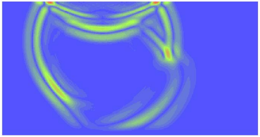

t=2.0 s

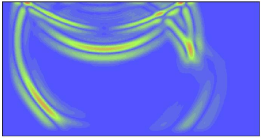

t=2.5 s

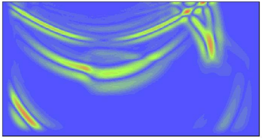

t=3.0 s

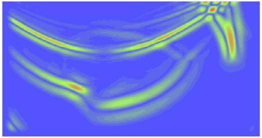

t=3.5 s

Seismic wave propagation: complex topography

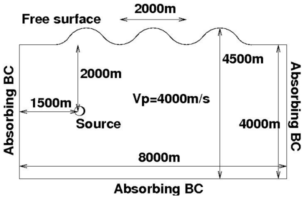

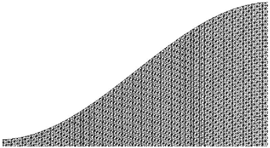
Mesh (zoom)

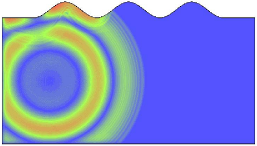
t=0.75 s

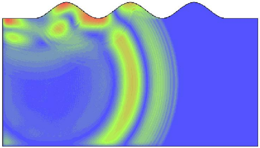
t=1.0 s

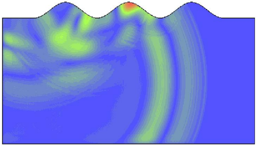
t=1.25 s

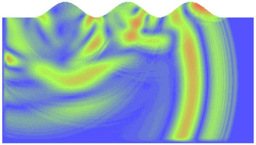
t=1.5 s

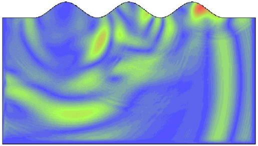
t=1.75 s

- Simulation of the spontaneous dynamic fault rupture
- Slip-weakning law
- Boundary conditions on the fault are deduced from an analysis of the total discrete energy
- M. Benjemaa, N. Glinsky-Olivier, V.M. Cruz-Atienza, J. Virieux and S. Piperno
  Dynamic non-planar crack rupture by a finite volume method
  Geophys. J. Int., Vol. 171, pp. 271-285, 2007

Rupture is 14.3 Km long with a 1 Km long nucleation zone
Contour lines of v_x (4 sec after rupture initiation)

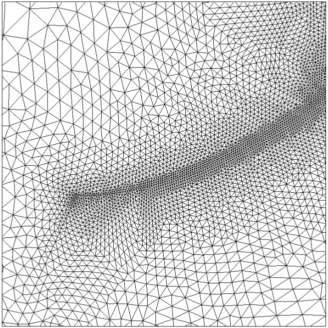

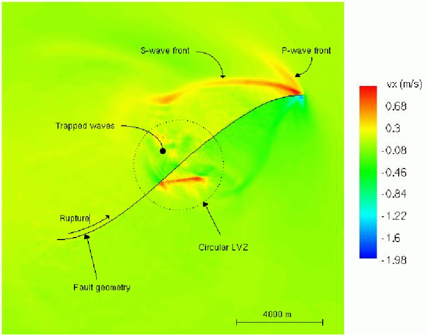

Parabolic fault geometry

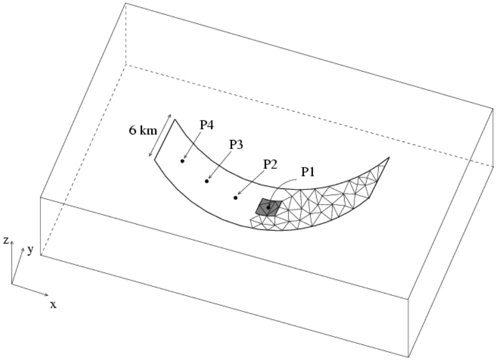

Numerical results: dynamic fault rupture
Propagation of a dynamic fault in 3D

Parabolic fault geometry

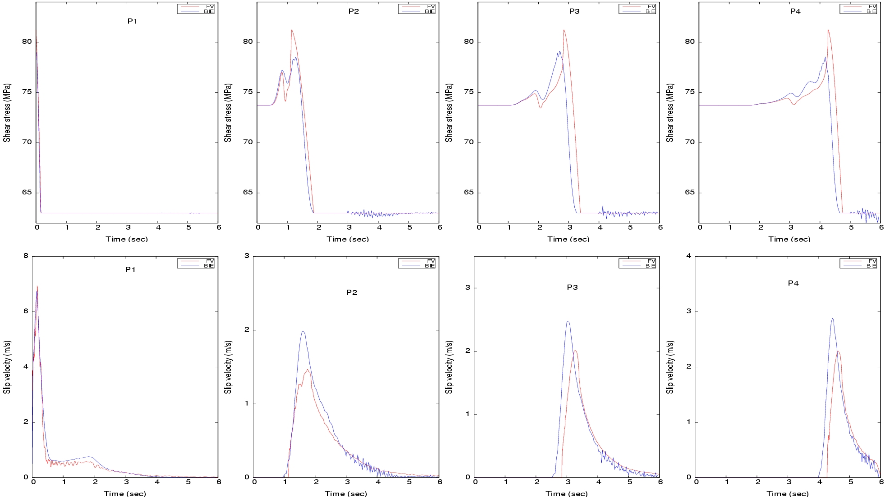

Parabolic fault geometry
Tetrahedral mesh: # vertices = 1,997,137 and # tetrahedra = 11,660,797
Physical time T=6.0 sec: 1360 sec on 64 AMD Opteron/2.0 GHz nodes with Gigabit Ethernet

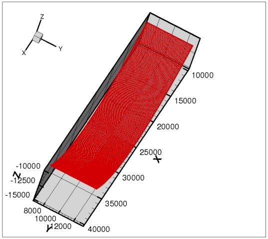

Surfacic mesh (fault only)

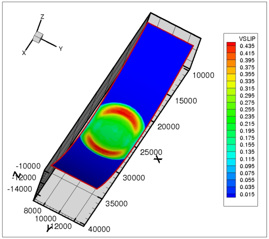

t=1.5 s

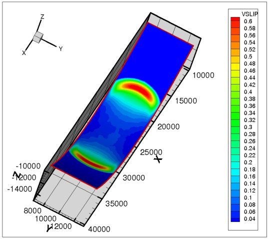

t=3.0 s

- Future works
  - High order $\mathbb{P}_p$-DG methods on tetrahedral meshes
  - p-adaptivity
  - Numerical treatment of viscoelastic material models with DG methods
  - Application to large-scale simulations of earthquake rupture process and generated ground motion

Closure

- Our contributions are before all concerned with methodological aspects
  - High-order discretization methods on unstructured meshes
  - Numerical treatment of complex material models
  - Parallel resolution algorithms
- Collaborations with physicists in related application domains are essential to our activities

Thank you for your attention!

Closure

- Our contributions are before all concerned with methodological aspects
  - High-order discretization methods on unstructured meshes
  - Numerical treatment of complex material models
  - Parallel resolution algorithms
- Collaborations with physicists in related application domains are essential to our activities

Thank you for your attention!